Chapter 4
AFM Imaging-Force Spectroscopy Combination for Molecular Recognition at the Single-Cell Level

Filomena A. Carvalho and Nuno C. Santos

Abstract Molecular recognition at the single-cell level is an increasingly important issue in Biomedical Sciences. With atomic force microscopy, cell surface receptors may be recognized through the interaction with their ligands, inclusively for the identification of cell-cell adhesion proteins. The spatial location of a specific interaction can be determined by adhesion force mapping, which combines topographic images with local force spectroscopy measurements. Another valuable possibility is to simultaneously record topographic and recognition images (TREC imaging) of cells, enabling the mapping of specific binding events on cells in real time. This review is focused on recent developments on these molecular recognition approaches, presenting examples of different biological and biomedical applications.

Intermolecular recognition may be considered as the beginning for many biochemical processes. It involves several types of forces between single molecules. Different approaches have been developed to measure intermolecular forces, such as optical trapping [1–3], pipette suction [4] and surface forces apparatus (SFA) experiments [5]. Optical trapping is a very sensitive technique, but it is limited to measurements of less than tens of piconewtons and can only be applied to a small group of samples. Pipette suction and SFA experiments are sensitive techniques, but both have poor spatial resolution. The use of atomic force microscopy (AFM) in this context may overcome the problems associated to the previous techniques.

AFM is a very powerful technique, with great spatial resolution, which can probe surfaces maintaining their physiological environments and measure forces down to the piconewton range [6–10]. AFM can be used not only for imaging but, since the mid 1990's, with the first force spectroscopy study [10, 11], it can also be used to record force-distance curves of biological systems. This enables AFM to measure

F. A. Carvalho (✉) · N. C. Santos
Instituto de Medicina Molecular, Faculdade de Medicina, Universidade de Lisboa, Lisbon, Portugal
e-mail: filomenacarvalho@fm.ul.pt

J. Cai (ed.), *Atomic Force Microscopy in Molecular and Cell Biology*,
https://doi.org/10.1007/978-981-13-1510-7_4

intermolecular forces between single molecules (*e.g.*, ligand-receptor interactions), which can be used for molecular recognition studies.

The combination of molecular recognition and topographic information has been studied by two different approaches: 1) adhesion force mapping mode, and 2) topographic and recognition (TREC) imaging.

1 Adhesion Force Mapping Using Force Spectroscopy

Adhesion force mapping can be performed by applying the force-volume mode or by collecting the topographic image with the maximum adhesion map on the retract part of a force-distance curve. On the force-volume mode, all force-distance curves are collected, leading to a huge amount of data, with difficult post-processing. The maximum adhesion map is created by recording whole force-distance curve(s) for every pixel of the scan. However, the ability to distinguish a molecule on the adhesion map is very limited as compared with the topography image; thus, usually no correlation between both images can be performed [12].

Force spectroscopy can be performed at a single sample spot, by selecting it on the AFM scanning image, or it can be record spatially in the x,y plane. Quantitative tip-sample adhesion maps may then be generated. The principle is to record spatially resolved force-distance curves by moving the AFM scanner across the biological samples over an area of a given size with n × n points to be probed (typically, 32, 64 or 128) [13–15]. The x,y AFM image is divided into a square grid of n^2 pixels and the system performs one or more approach/retract cycle(s) on the center of each square/pixel, with a common lateral resolution from a few tens to hundreds of nanometers per pixel (Fig. 4.1) [16]. At the same time, the system creates maps (of height, adhesion or elasticity), which data may be processed and quantified. Thus, for each force-distance curve, a given property of the sample can be extracted, quantified and displayed on maps. Color or grey scale can be used to display the pixels on the maps of each analyzed property of the sample. Brightness pixels reflect the magnitude of the measured property at a defined location [17–20]. Due to speed limitations and poorer spatial resolution on the most common atomic force microscopes, this method did not have significant scientific progress before the 2000's. Only after 2001, with the development of high-speed scanners, free of resonant vibrations up to 60 kHz, it was possible to build a high-speed AFM. This microscope was capable to capture a 100 × 100 $pixel^2$ images within 80 ms and, therefore, generate a movie of biological samples under physiological conditions [21]. This AFM provided a way to record and correlate data from structure, adhesion and elasticity maps of samples faster, achieving molecular resolution.

In 2008, Sahin et al. conducted a nanomechanical mapping by the real-time analysis of time-varying tip-sample forces in tapping-mode AFM [23]. For the first time, they constructed maps of local elastic modulus and adhesion forces, together with conventional phase and topography images, in tapping mode. This new approach allowed the nanomechanical analysis of samples with gentle forces and high spatial

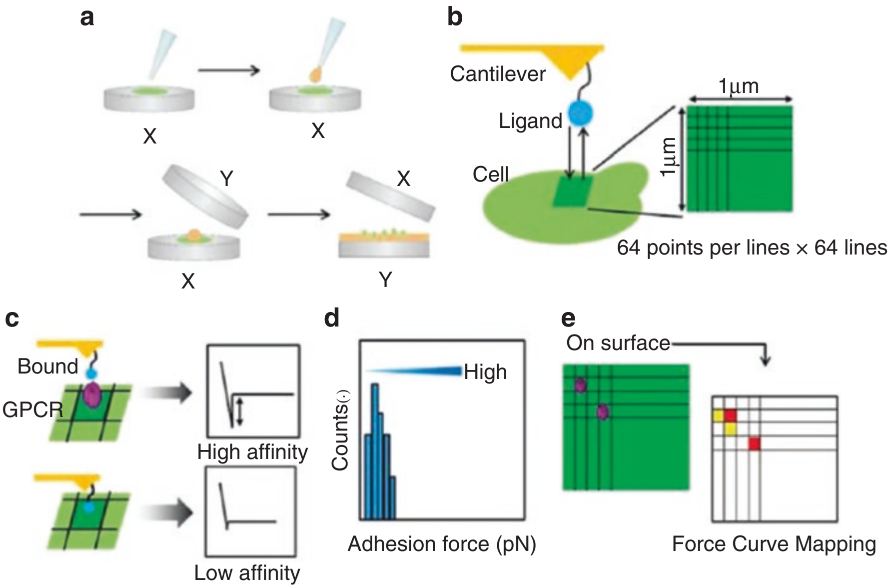

Fig. 4.1 Schematic representation of adhesion force mapping. (**a**) Immobilization procedure for a sample on a glass slide. (**b**) A cantilever derivatized with a ligand approaches to the surface of a cell to conduct force measurements of n × n points within 1 × 1 μm^2. (**c**) Differences between high and low affinity systems. (**d**) Adhesion force histogram. (**e**) Force curve adhesion mapping, representing high (*red*), low (*yellow*) and very low (*white*) affinity binding measurements. Reprinted with permission from [22]

resolution [23]. A new dynamic AFM method to quantitatively map the nanomechanical properties of live cells with a throughput 10 to 1000 times higher than that achieved with quasi-static AFM techniques was introduced in 2011 [24]. In 2015, a new fast scanning quantitative dynamic AFM method for nanomechanical imaging of heterogeneous live cells in solution was introduced, using the cantilever mean deflection as feedback signal, instead of standard amplitude reduction. This new method was able to achieve a 10 to 20-fold improvement in imaging throughput, compared to amplitude-modulation AFM [25].

Moreover, combining force spectroscopy mapping with an AFM-mounted fluorescence microscope enables dual fluorescence and AFM adhesion map imaging, allowing the detection and local determination of potential submicron-sized adhesive regions [26]. Nanoparticle tracking analysis and quantitative nanomechanical mapping AFM were also combined to determine size and nanomechanical properties of exosomes isolated from non-malignant and malignant (metastatic and non-metastatic) cell lines [27]. Authors revealed that malignant cell line exosomes have lower stiffness and adhesion compared to non-malignant cell line exosomes.

AFM-based adhesion nanomechanical mapping provides insights into the functions of different biological systems [28]. This technology has already been applied by different researchers to simultaneously image and quantify biophysical properties of complex samples, such as diatoms [29], lipid phases in supported bilayers [30], diverse membrane proteins [31–33], yeasts [34], virus capsids [35], human cells [25, 36–40] and neurodegenerative amyloid fibrils [41].

In 1998, Willemsen et al. demonstrated that the resolution of the topographical image in adhesion mode is only limited by tip convolution and, thus, comparable to tapping mode images. By comparing the high-resolution height image with the adhesion image, it is possible to show that specific molecular recognition is highly correlated with topography. This was possible by studying recognition events for individual antibody-antigen pairs when authors imaged individual ICAM-1 antigens both in tapping mode and the adhesion mode [42].

The characterization of the local mechanical properties of polymer cushioned membranes [43], as well as nanofibers [44], was also possible by applying force mapping methodologies. An AFM tip functionalized with cytochrome C2 molecules was also used to map native protein-protein interactions found in bacterial photosynthesis (electron donor/intrinsic membrane acceptor pair) [45]. AFM was also used to measure the adhesion force between targeting receptors and their ligands, and to map the targeting receptors (*e.g.*, Ste2p, a G protein-coupled receptor [22]). At the level of protein-protein interactions, the measurement of the binding force between glyceraldehyde-3-phosphate dehydrogenase (GAPDH) and Ras homologue enriched in brain (Rheb) was also performed [46]. By AFM-recognition mapping using specific DNA aptamers, it was possible to study the binding between human α-thrombin and vascular endothelial growth factor (VEGF), two proteins involved on the clotting cascade [47]. It is therefore possible to generate high resolution maps to spatially and temporally identify proteins at the molecular level on complex surfaces.

On other fields of research, such as crime scene investigations, PeakForce quantitative nanomechanical mapping (PF QNM) AFM has been used to study the variations in surface adhesion and topography of latent fingermark droplets over time [48].

On this review, we will highlight the application of adhesion force mapping methodologies to study different types of cells.

In 2015, Rigato et al. performed AFM-based mechanical mapping on cells plated on micropatterns, demonstrating a pattern-specific reproducible mechanical response [49]. This yields the possibility of average the data of the elasticity maps allowing to specifically locate intracellular elasticity differences, which are maintained among cells, and to identify regions characterized by higher or lower mechanical stability [49].

One of the first studies that was performed with microbial cells was done by Gad et al. [20], whom focused on the distribution of mannan, a particular type of polysaccharides, on the surface of a living microbial cell. Specific AFM mapping molecular recognition events were only detected on specific areas of the cell surface, which was interpreted as reflecting a non-uniform distribution of mannan on the cell surface. Specific procedures are necessary to conduct these AFM measurements. Methods for: (i) functionalizing AFM tips with *Pseudomonas aeruginosa* or concanavalin A, (ii) for stretching specific polysaccharide molecules on live bacteria using single-molecule force spectroscopy with lectin-coated tips, and (iii) for mapping the localization, adhesion and extension of individual polysaccharide chains were described in detail [50].

Experiments to measure the interaction forces of bacterial adhesins (HBHA) and for assessing their distribution on the surface of living cells (*Mycobacterium bovis* BCG cells) were successfully conducted by Dupres et al. [19, 51]. High-resolution image and adhesion force maps of a sodium dodecyl sulphate-treated *Aspergillus fumigatus* spore revealed high correlation between structural and hydrophobic heterogeneities [52].

In 2013, Alsteens et al. reported the correlation between structural, adhesion and elasticity images of complex biological samples, recorded at high temporal and spatial resolutions, and with biochemical specificity [18]. Using this method, they provided a direct visualization of the assembly machinery of bacteriophages on living cells, revealing that they localize near the septum, in the form of soft nanodomains surrounded by stiffer cell wall material [18]. The assessment of the electric charge distribution on the surface of the cell wall of Gram-positive bacteria was also proven to be feasible by AFM mapping images at a spatial resolution better than a few tens of nanometers [53].

On another report, the hydrophobic forces engaged in Epa6-mediated cell adhesion were successfully measured by AFM [54]. Using single-cell force spectroscopy, the authors conclude that *Candida glabrata* wild-type (WT) cells bind to hydrophobic surfaces via strongly adhesive macromolecular bonds, while mutant cells with impaired in Epa6 expression are weakly adhesive (Fig. 4.2).

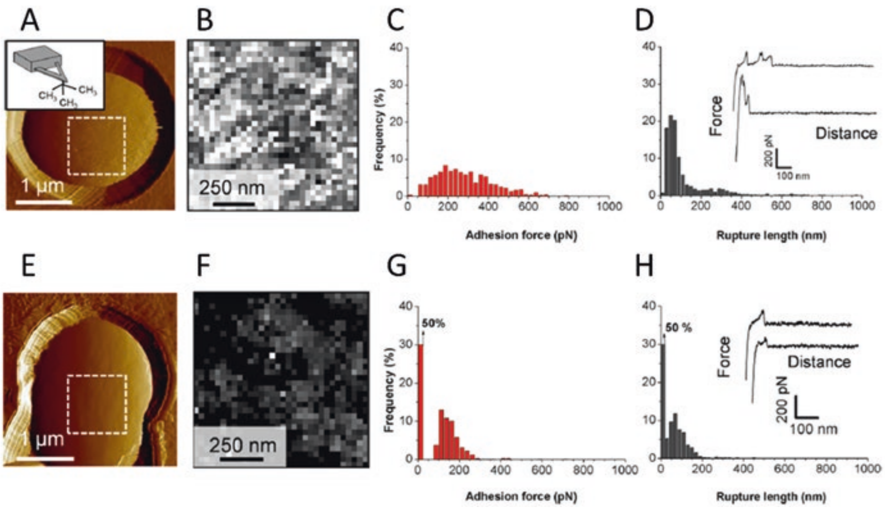

Fig. 4.2 Mapping and quantification of hydrophobic forces on *C. glabrata* cells using chemical force microscopy. AFM deflection images of WT (**A**) and Epa6 mutant (**E**) cells. The dashed white squares indicate the regions where the force maps were recorded. Adhesion force maps (1 µm × 1 µm; bright pixels correspond to hydrophobic binding events) of WT (**B**) and mutant (**F**) cells; respective adhesion force (**C**, **G**) and rupture length (**D**, **H**) histograms. Adapted and reprinted with permission from [54]

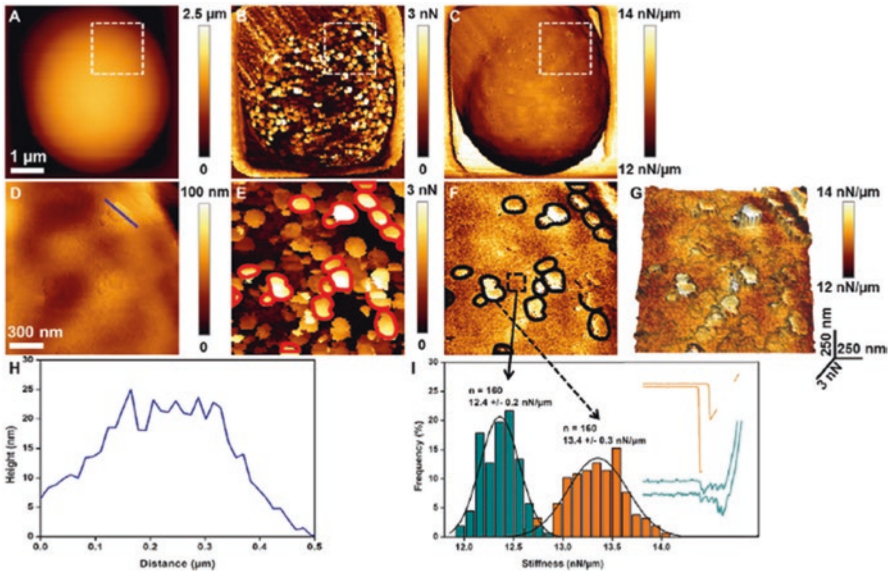

Fig. 4.3 Nanomechanics of the adhesive domains of *C. albicans* cells. Height image (**A**), and corresponding adhesion (**B**) and stiffness (**C**) images. Height (**D**), adhesion (**E**) and stiffness (**F**) images of a small area on top of the cell, corresponding to the white dashed square on A. Adhesive nanodomains circled in red on (**E**) are also found on the stiffness image (black circles on (**F**)). 3D-image of the adhesion mapped with the stiffness (**G**). Cross-section (**H**) taken along the blue line on (**D**). Distribution of the stiffness values (**I**) corresponding to the cell wall and the less adhesive domains (blue columns) or to the most adhesive domains (orange columns). Reprinted with permission from [55]

The observation that adhesins at the surface of *Candida albicans* cells are organized in nanodomains composed of free or aggregated mannoproteins was possible by AFM mapping of the adhesive properties of these cells (Fig. 4.3) [55].

Using a dynamic AFM technique operating in the intermittent contact regime to quantitatively map the local electro-mechanical force gradient, adhesion, and hydration layer viscosity within individual f29 virions, other authors provided new evidences of how bacteriophages like pressurized vessels, releasing DNA through any fracture present on the viral shell [56].

By studying the effect of plasma membrane receptor clustering on local cell mechanics, Almqvist et al. obtained adhesion force maps for the interaction between an antibody at the AFM tip and a specific VEGF receptor [17]. VEGF receptors were found to concentrate toward the cell boundaries and cluster rapidly, with local stiffness reductions (Fig. 4.4).

Mapping images of the distribution of sugar chains on epithelium and of the receptor associated protein (RAP) binding proteins on fibroblasts were also obtained [57, 58].

In 2007, the local mechanical characteristics of different cell types (namely, muscle, endothelial, epithelial and glial cells, neurons, fibroblasts, osteoblasts,

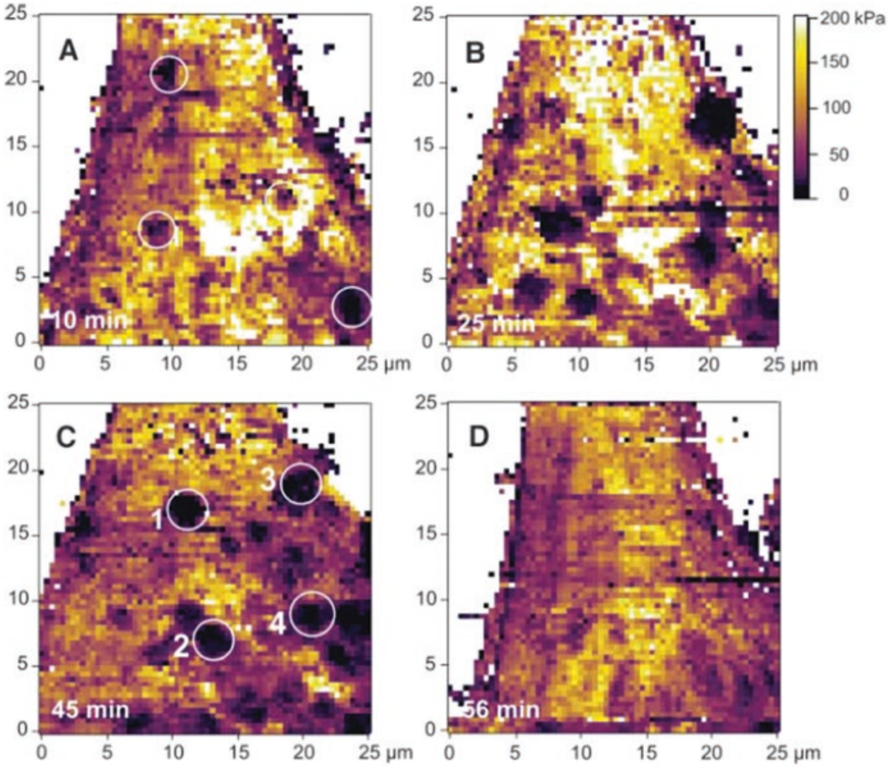

Fig. 4.4 Elasticity maps of the evaluated Young's modulus on endothelial cells in real-time, showing clustering of VEGF receptors on the cell surface. Images are colour-coded according to the bar, from 0 kPa (*dark*) to 200 kPa (*bright yellow*). Images show the elasticity at different time points after adding anti-flk-1 antibody: 10 min (**A**), 25 min (**B**), 45 min (**C**) and 56 min (**D**) after addition. A few regions with lower elasticity are marked with numbers 1–4 in (**C**). The regions underlying the receptor clusters appeared as less stiff. Reprinted with permission from [17]

blood cells and sensory cells) were analysed by Kuznetsova et al. [59]. According to this work, normal cells are one order of magnitude stiffer than cancer cells. Authors suggested that such change in elastic properties might be attributed to a difference in cytoskeleton organization. In another study, mapping of the local Young's modulus of a living astrocytes revealed that stiffer areas correspond to the sites where the cytoskeleton fibers are located (Fig. 4.5) [60].

Cassina et al. demonstrated that a peptide obtained from the cleavage of the neuroprotein VGF stimulates intracellular calcium mobilization in Chinese Hamster Ovary (CHO) cells [61]. The sub-cellular localization of the tyrosine kinase receptor (Met) for hepatocyte growth factor on hippocampal neurons was also studied by AFM force spectroscopy adhesion mapping. Authors found that multimeric activated Met is concentrated in the dendritic compartment, while the inactivated monomeric form of Met was prominent on the soma [62]. An adhesion force

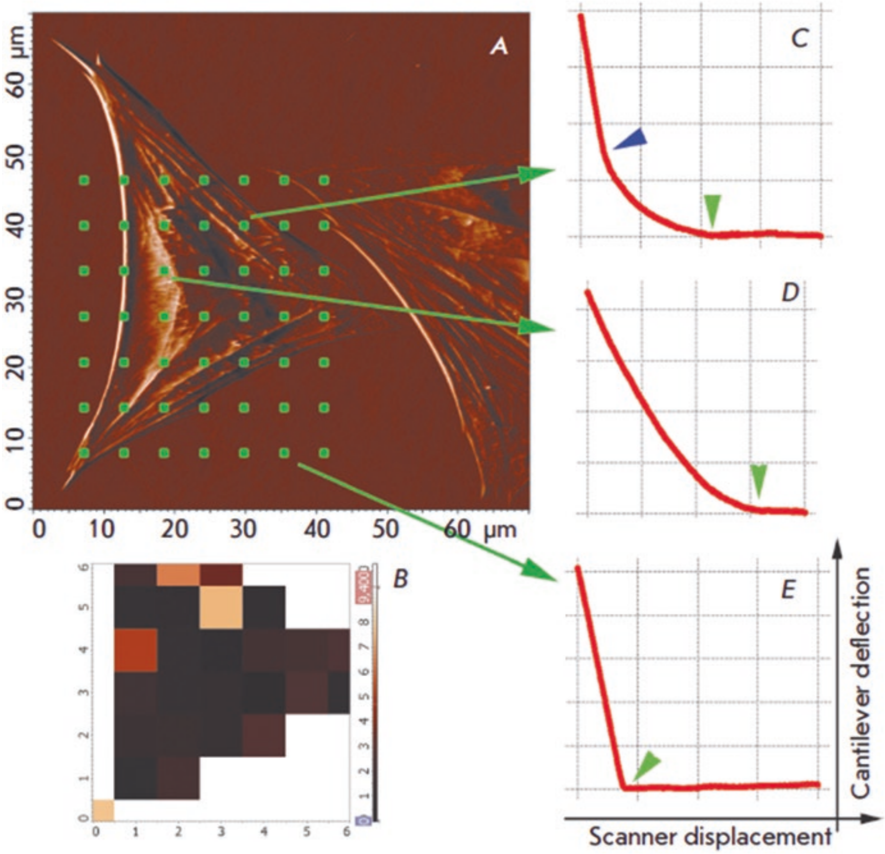

Fig. 4.5 Mapping the local Young's modulus of astrocytes. (**A**) Deflection image of a living astrocyte, with a grid of points indicating where the force curves were obtained. (**B**) Map of the local Young's modulus in the grid nodes (colour scale in kPa, with lighter squares corresponding to stiffer areas). (**C**) Force curve obtained in a point above the cell edge; the upper part of the curve coincides with the curve obtained on the substrate (**E**). Green arrows mark the contact point and the blue arrow the point where the cantilever touches the substrate. (**D**) Force curve obtained in a point above the cell nucleus. Reprinted with permission from [60]

mapping methodology was also applied to reveal the nanoscale distribution of Fc gamma receptors on local areas of macrophages, which have an important role in clinical cancer immunotherapy [38].

The morphology and the elastic properties of live cultured, non-malignant human mammalian epithelial cells (HMEC) and cancerous breast epithelial cells (MCF7) were also investigated through AFM force mapping [40]. The quantification of the surface density and the spatial organization of CXCR4 on breast cancer cell membranes were also assessed by AFM, leading the authors conclude that the CXCR4 density, spatial organization, and matrix stiffness are paramount to achieve strong binding [63].

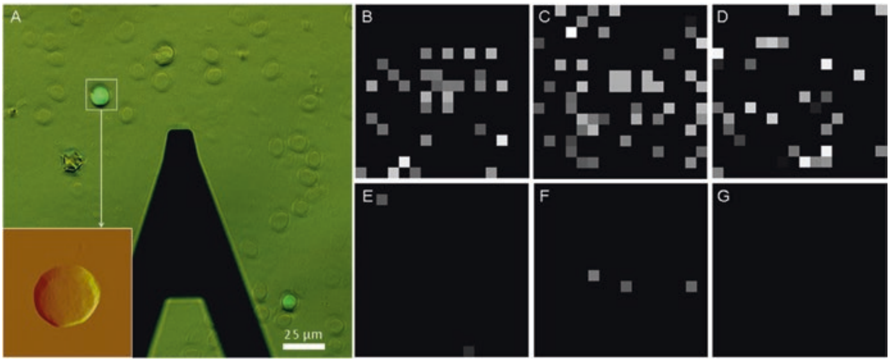

Fig. 4.6 Detection of specific CD20-rituximab interactions on cancer cells. (**A**) Fluorescence image of a clinical bone marrow cell sample, with the AFM image of a single cell as inset. (**B, C, D**) CD20 distribution maps on the cancer cells. (**E, F, G**) CD20 distribution maps on the cancer cells after blocking with rituximab, a monoclonal antibody against CD20. Grayscale is from black to white, up to 200 pN. Reprinted with permission from [39]

Specific molecular-receptor interactions on living human colorectal cancer cells were also already tested as *in vitro* models for gut epithelium [36]. On this study, authors measured the binding of wheat germ agglutinin to the surface of living Caco-2 human intestinal epithelial cells.

Using fast scanning dynamic AFM, it was possible to observe the nanomechanical spatio-temporal response of the cortical actin cytoskeleton, including the formation and movement of lateral actin bands [25]. These bands are characteristic of the retrograde actin flow machinery rapidly formed by inhibiting Syk expression in MDA-MB-231 breast cancer cells.

AFM was also applied to map the nanoscale distribution of CD20 molecules on the surface of cancer cells from clinical B-cell non-Hodgkin's lymphoma (NHL) patients, with the assistance of ROR1 (a cell surface marker expressed exclusively on cancer cells) fluorescence recognition (Fig. 4.6) [39]. The membrane protein CD20 is an effective target for treating B-cell NHL, as demonstrated in clinical practice. That study provided a new approach to directly investigate the nanoscale distribution of a target protein on individual clinical cancer cells.

2 Topographic and Recognition (TREC) Imaging

The second approach to study molecular recognition is a very powerful technique, which combines imaging at high resolution and single-molecule interaction measurements [64–66]. TREC imaging is a dynamic approach that uses an oscillating tip close to its resonant frequency [65, 67]. This technique is faster and has better lateral resolution (few nanometers) than adhesion force mapping [15, 65, 66]. Topographic and recognition images are obtained at the same time, allowing to distinguish sites of receptors in the recognition image, spatially correlating them with features of the topographic image. TREC imaging uses a molecule (ligand) covalently attached to the AFM tip, usually via a flexible crosslinker (*e.g.*, poly(ethylene glycol) – PEG) [68–70]. During the scanning of the surface, the functionalized tip oscillates close to its resonance frequency. The binding sites are evident from the reduction in the oscillation amplitude, as a result of specific recognition during the lateral scan. Enhanced signal processing, in combination with a modified feedback loop [64], provides a recognition image simultaneously acquired alongside the topography image. The separation of topographical and recognition signals is achieved by splitting the cantilever's oscillation amplitude into lower and upper parts (relative to the cantilever's resting position), containing solely topography and recognition information, respectively. The maxima of these parts are then used to record the topography (lower part) and recognition image (upper part) at the same time (Fig. 4.7) [71, 72].

TREC imaging on AFM offers different advantages [73]: (i) high resolution of samples and high tracking capacity of target molecules on cells; (ii) high recognition specificity; (iii) less sample damage and no sample pre-treatment; and, (iv) simple and clear output, demonstrating the exact location of target molecules on the surface of the scanned sample. The use of TREC imaging offers a wide range of biological applications. It enables the study of the real location of single molecules on a tissue or cell surface, providing new perceptions of cell physiological mechanisms.

Applying TREC imaging, it is possible to investigate interactions of single molecules with their specific receptors, while simultaneously recording a high-resolution topography image. The combination of topographic and recognition images has been demonstrated on different biological systems with great success. This technique has already been useful to study chromatin structures [65], receptor-ligand pairs [64, 66, 72], proteins [75], isolated erythrocyte membranes [76] and cells [77, 78].

Radmacher et al. reported one of the first adhesion mapping studies, which was done by mapping lysozyme aggregates adsorbed onto mica [79]. A decrease of the adhesion of the tip with the lysozyme compared to mica was observed. This study was performed with a non-functionalized tip and the adhesion map was based on the physicochemical properties of the molecule and the substrate, rather than on specific biomolecular interactions. Ludwig et al. used a biotin-functionalized tip to map a streptavidin pattern and, with specific high-affinity interaction measurements, were able to create an adhesion map [80].

In 2005, Agnihotri et al. used binary recognition images to differentiate specific from unspecific interactions between fibrinogen on the surface and its specific antibody [81]. The number of recognition events had a major decrease after blocking the surface with anti-fibrinogen antibodies. The positive events observed in the recognition image were considered as specific antibody-fibrinogen interactions.

An adaptation of this technique was proposed by Wang et al. which used an AFM tip with two tethered antibodies and sequential blocking to identify two types of proteins in single AFM images of compositionally complex molecules [82]. By

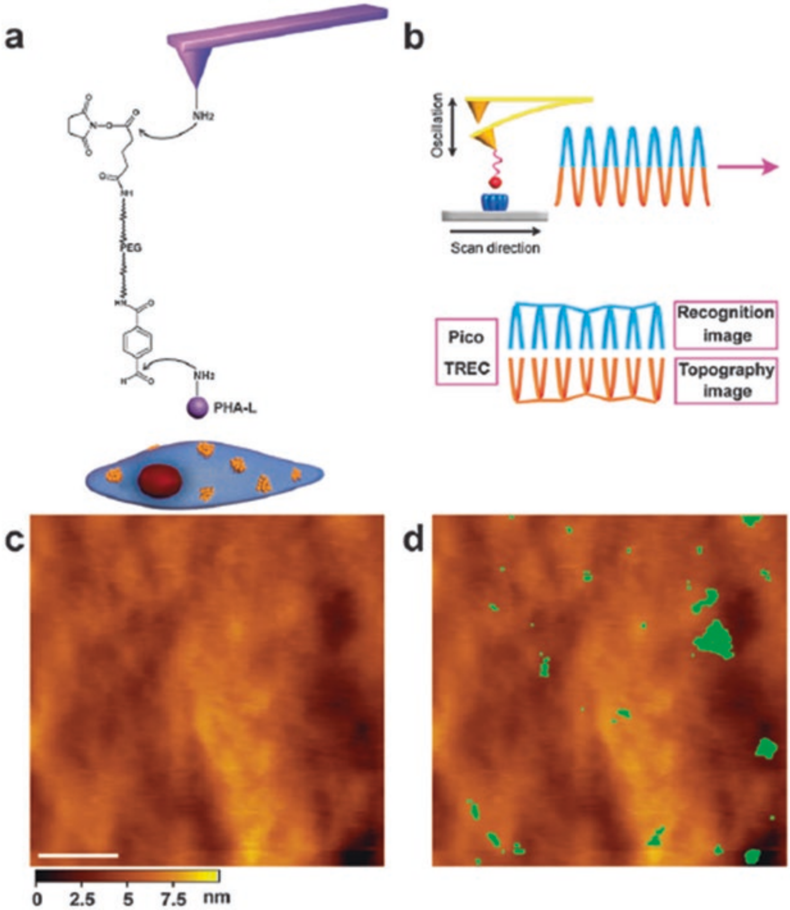

Fig. 4.7 TREC molecular recognition imaging of galactose on the surface of HeLa cells. (**a**) Scheme of the AFM tip modified with a lectin (PHA-L). (**b**) Principles of TREC imaging, scanning the cell with the modified tip (scale bar: 300 nm). (**c**) Topography image. (**d**) Topography image with the recognition signal superimposed. Adapted and reprinted with permission from [74]

applying this methodology, authors were able to analyse two specific components, BRG1 and β-actin, of the human Swi-Snf ATP-dependent nucleosome remodelling complex and two types of histones, H2A and H3, on the chromatin samples (Fig. 4.8).

Sotres et al. proposed other mode of performing force scanning by AFM, named jumping mode [12]. Topographic and tip-sample adhesion maps are acquired simultaneously. Lateral resolved adhesion maps of avidin-biotin unbinding forces highly correlated with single avidin molecules in the corresponding topographic map were achieved after testing this method.

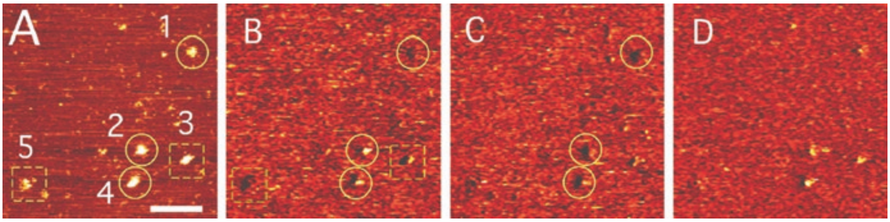

Fig. 4.8 Identification of different subunits in a multiprotein complex. Human Swi-Snf ATP-dependent nucleosome remodelling complexes were deposited and scanned with an AFM tip with both anti-BRG1 and anti-β-actin antibodies, rescanned in the presence of β-actin blocking peptide, and then rescanned in the presence of BRG1 and β-actin blocking peptides. (**A**) Topographic image from the initial scan. (**B**) Corresponding recognition image (no blocking). (**C**) Recognition image obtained after blocking with β-actin peptide. (**D**) Recognition image obtained when both BRG1 and β-actin blocking peptides are present. Dashed squares identify complexes whose recognition disappears after blocking with β-actin peptide and solid circles identify complexes whose recognition disappears only when BRG1 blocking peptide is present. Squares and circles are shown only when molecular recognition occurs, *i.e.*, in (**B**) and (**C**). Reprinted with permission from [82]

A simple procedure for adjusting the optimal amplitude for TREC imaging was described by Preiner et al. [71]. This method takes advantage of the sharp localization of the TREC signal within a small range of oscillation amplitudes. Using this procedure, authors imaged single avidin molecules immobilized on a mica substrate with an AFM tip functionalized with a biotinylated IgG.

In 2014, van Es et al. presented a new way to look at AFM TREC data. TREC imaging was used on a model system comprising an S-layer surface modified with Strep-tag II for binding sites and Strep-Tactin bound to the AFM tip [83]. They have shown that high resolution TREC images contain information on binding and unbinding rates for surface bound molecules. They also presented a method to analyse the TREC images to extract these rates as a function of distance between the AFM tip and the binding site. The authors concluded that high resolution TREC imaging is a valid method to determine k_{on} values at the single-molecule level [83].

Force clamp force mapping (FCFM), an AFM-based technique for measuring the viscoelastic creep behaviour of live cells with sub-micrometer spatial resolution, can also be successfully applied [84].

A study from 2009 evaluated the changes in surface topography, surface adhesion, indentation depth and Young's modulus on a metal-tolerant marine bacterium after its exposure to cobalt (II) ions [85]. An overall increase on the elasticity of the bacterial membrane and an increase in adhesiveness were observed.

Detailed procedures for all stages of TREC experiments with cells (*e.g.*, vascular endothelial cells), from tip and sample preparations to the operating principles and visualization, were described by Chetcheglova et al. [86].

The distribution of osteopontin (OPN) over pre-osteogenic cell membrane was tracked by mapping the adhesion forces between an anti-OPN coated probe and the cell surface. Authors were able to recognize specific OPN nanodomains on the cell membrane (Fig. 4.9) [73].

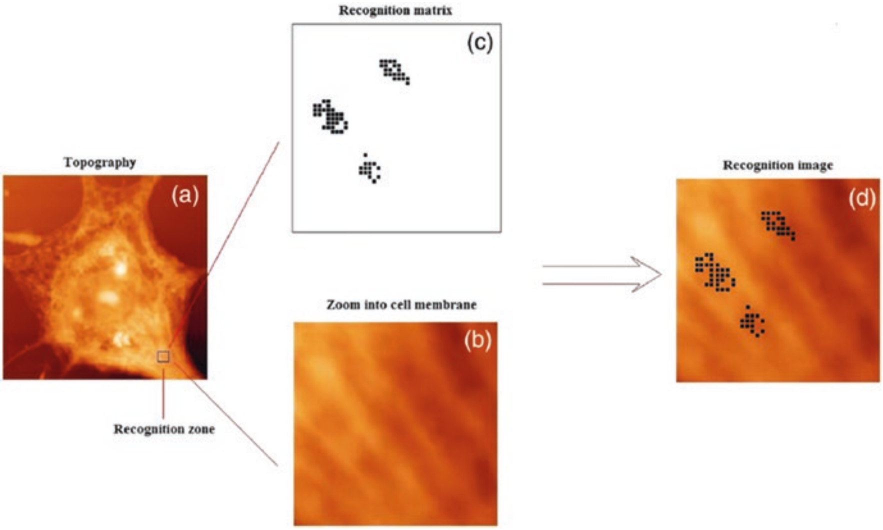

Fig. 4.9 (**a**) Topographic AFM image of a pre-osteogenic cell (the black frame on the right corner shows the chosen recognition zone). (**b**) High resolution topography image of the recognition zone. (**c**) Recognition matrix demonstrates the location of all specific binding events between anti-OPN tip and the OPN proteins on the cell surface. (**d**) The recognition image was created by merging the binary matrix image (**c**) and the high resolution topography image of the recognition zone (**b**). The image reveals the location of all OPN sites over the recognition zone. Each black square indicates the location of an OPN site. AFM images of 30 × 30 μm^2 (**a**) and 1 × 1 μm^2 (**b**–**d**). Reprinted with permission from [73]

On another TREC imaging study, galactose was detected and localized on the surface of cancer and normal cells [74]. Authors revealed that there are more galactose residues on cancer cells than on normal ones, and that the stability of galactose-lectin binding on cancer cells is much lower than that on normal cells.

Recently, the interaction of the specific DNA aptamer sgc8c immobilized at the AFM tip with its corresponding receptor, protein tyrosine kinase-7 (PTK7), embedded in the membrane of acute lymphoblastic leukaemia (ALL) cells (Jurkat T-cells) was investigated [87]. A homogeneous distribution of PTK7 molecules on the outer regions of ALL cells with a surface density of 325 ± 12 PTK7 receptors (or small receptor clusters) per μm^2 was demonstrated (Fig. 4.10).

TREC mapping was also applied to the imaging of α actinin-4 filaments and mapping of the epitopic region within α actinin-4 molecule using an antibody functionalized tip [88]. To gain a comprehensive view of the structural and chemical properties of *Staphylococcus epidermidis*, four different strains (biofilm positive and biofilm negative strains) were also analysed using the same methodology [89]. On this study, force measurements performed using bare hydrophilic silicon nitride tips disclosed similar adhesive properties for each strain. However, the use of hydrophobic tips showed that hydrophobic forces are not the driving forces for adhesion

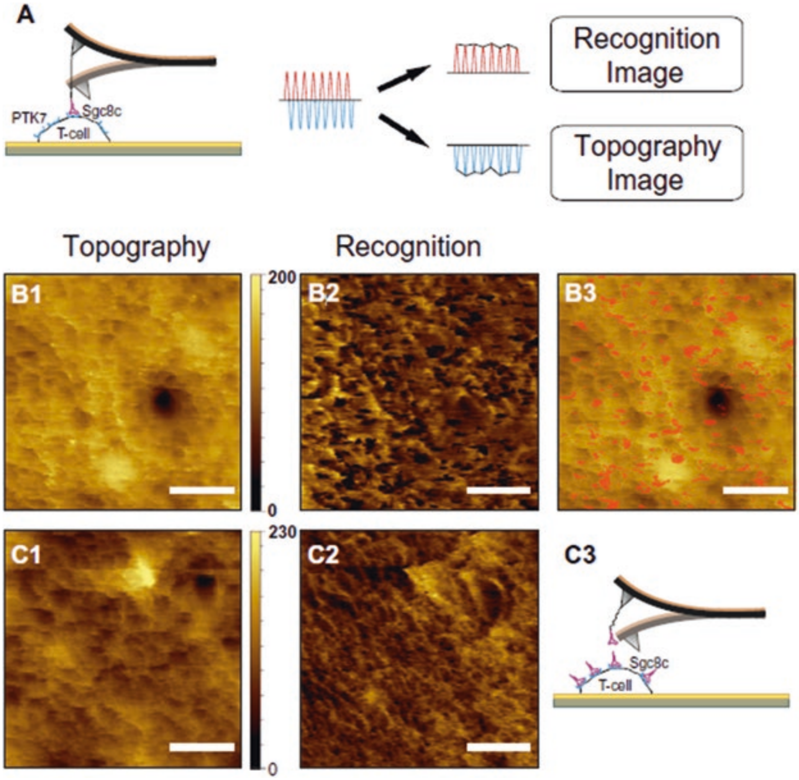

Fig. 4.10 (**A**) Schematic representation of the TREC setup. Simultaneously acquired topography (**B1**) and recognition (**B2**) images on a T-cell membrane using sgc8c functionalized tips. A superimposition of topography and recognition is also shown (**B3**). After addition of free aptamers, the topography image (**C1**) remains unchanged, whereas the recognition spots (**C2**) are completely abolished, as a result of blocked PTK7 receptors, as illustrated in (**C3**). Scale bars: 500 nm. Reprinted with permission from [87]

of the four strains. Treatment of two biofilm positive strains with two chemical inhibitor compounds leads to a loss of adhesion, suggesting that AFM could be a valuable tool to screen for anti-adhesion molecules.

Studying the binding affinity of peptides binding to various materials is also possible with quantitative force mapping methods [90].

TREC can be combined with other techniques. One example of this was presented by Zhu *et al.*, which used native-protein nanolithography (NPNL) and TREC to synergistically use AFM tips to write and image nanoscale protein patterns on a surface [91]. The approach was validated using surface-bound biotinylated bovine serum albumin (BSA) and AFM tips carrying streptavidin tethered via a flexible PEG linker. Another example is the combination of AFM with scanning electrochemical microscopy (SECM) in peak force tapping (PFT) mode, thereby offering spatially correlated electrochemical and nanomechanical information paired with high-resolution topographical data under force control [92]. The development of this approach may also be used to study complex biological samples, such as bacterial cells. Hinterdorfer et al. have shown that AFM combined with near-field scanning optical microscopy (NSOM) provide a broad range of possibilities for mapping the distribution of single molecules on the surfaces of cells with nanometer spatial resolution, thereby shedding new light on their highly sophisticated functions, namely on the study of the adhesion of *C. albicans* to proteins (Fig. 4.11) [93, 94].

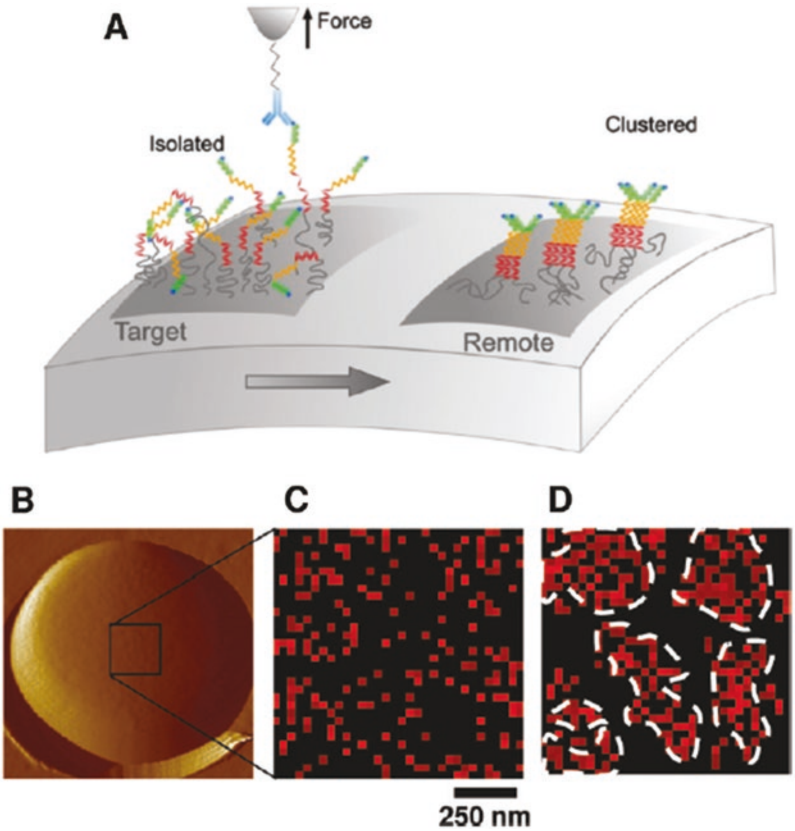

Fig. 4.11 Single-molecule AFM imaging unravels the dynamic clustering of cell adhesion proteins on yeast cells. (**A**) Single Als proteins from *C. albicans* were localized and stretched using an AFM tip bearing specific antibodies. (**B**) AFM topographic image of a single live cell. (**C**) Adhesion force map recorded on a cell that was never subjected to force. Red pixels document the detection of single proteins. Most proteins were isolated and evenly distributed, without any clear evidence for clustering. (**D**) Subsequent mapping recorded on the same cell after mechanical stimulation. Unlike native cells, cells that had been preactivated by force displayed adhesion nanodomains referred to as “nanoadhesomes” (**A**). Reprinted with permission from [93, 94]

3 Conclusions

The molecular recognition of the specific interactions between two molecules, proteins, membranes, or the entire surface of cells is essential to understand both structure and function(s). The recent advances on single-molecule imaging approaches, as for atomic force microscopy, allowed researchers to take advantages of these methods, with high improvements in spatial/temporal resolution, cell imaging speed, ease of use, higher throughput analysis and maintenance of *in vivo* cell physiological conditions.

Here, two different methods that combine AFM imaging and force spectroscopy were explained in detail: adhesion force mapping and TREC imaging. Both methods have expanded AFM beyond basic imaging studies, giving researchers the possibility to record and correlate data from structure, adhesion and elasticity maps, as well as to quantify molecular recognition events on different biological samples. Several applications of both methods led to numerous discoveries in cell biology, immunology, pharmacology and medical field. Some of the most recent studies are compiled on this review. We believe that the evolution and extension of the use of both methods will lead to important scientific discoveries and future developments in Biology and Medicine.

Acknowledgements This work was funded by Fundação para a Ciência e a Tecnologia – Ministério da Ciência, Tecnologia e Ensino Superior (FCT-MCTES, Portugal) projects PTDC/BBB-BMD/6307/2014 and PTDC/BBB-BQB/3494/2014.

Conflict of Interest Disclosures The authors declare no competing financial interests.

References

1. Ashkin A, Dziedzic JM, Yamane T. Optical trapping and manipulation of single cells using infrared laser beams. Nature. 1987;330(6150):769–71. https://doi.org/10.1038/330769a0.
2. Kuo SC, Sheetz MP. Force of single kinesin molecules measured with optical tweezers. Science. 1993;260(5105):232–4.
3. Svoboda K, Schmidt CF, Schnapp BJ, Block SM. Direct observation of kinesin stepping by optical trapping interferometry. Nature. 1993;365(6448):721–7. https://doi.org/10.1038/365721a0.
4. Evans E, Berk D, Leung A. Detachment of agglutinin-bonded red blood cells I forces to rupture molecular-point attachments. Biophys J. 1991;59(4):838–48. https://doi.org/10.1016/S0006-3495(91)82296-2.
5. Israelachvili JN. Force-measuring techniques. In: Intermolecular and surface forces. 3rd ed. San Diego: Academic; 2011. p. 223–52. https://doi.org/10.1016/B978-0-12-375182-9.10012-0.
6. Dammer U, Hegner M, Anselmetti D, Wagner P, Dreier M, Huber W, Guntherodt HJ. Specific antigen/antibody interactions measured by force microscopy. Biophys J. 1996;70(5):2437–41. https://doi.org/10.1016/S0006-3495(96)79814-4.
7. Florin EL, Moy VT, Gaub HE. Adhesion forces between individual ligand-receptor pairs. Science. 1994;264(5157):415–7.

8. Hinterdorfer P, Baumgartner W, Gruber HJ, Schilcher K, Schindler H. Detection and localization of individual antibody-antigen recognition events by atomic force microscopy. Proc Natl Acad Sci U S A. 1996;93(8):3477–81.
9. Lee GU, Kidwell DA, Colton RJ. Sensing discrete streptavidin-biotin interactions with atomic force microscopy. Langmuir. 1994;10(2):354–7. https://doi.org/10.1021/la00014a003.
10. Moy VT, Florin EL, Gaub HE. Intermolecular forces and energies between ligands and receptors. Science. 1994;266(5183):257–9.
11. Ishijima A, Doi T, Sakurada K, Yanagida T. Sub-piconewton force fluctuations of actomyosin in vitro. Nature. 1991;352(6333):301–6. https://doi.org/10.1038/352301a0.
12. Sotres J, Lostao A, Wildling L, Ebner A, Gomez-Moreno C, Gruber HJ, Hinterdorfer P, Baro AM. Unbinding molecular recognition force maps of localized single receptor molecules by atomic force microscopy. ChemPhysChem. 2008;9(4):590–9. https://doi.org/10.1002/cphc.200700597.
13. Grandbois M, Dettmann W, Benoit M, Gaub HE. Affinity imaging of red blood cells using an atomic force microscope. J Histochem Cytochem. 2000;48(5):719–24. https://doi.org/10.1177/002215540004800516.
14. Heinz WF, Hoh JH. Spatially resolved force spectroscopy of biological surfaces using the atomic force microscope. Trends Biotechnol. 1999;17(4):143–50.
15. Hinterdorfer P, Dufrene YF. Detection and localization of single molecular recognition events using atomic force microscopy. Nat Methods. 2006;3(5):347–55. https://doi.org/10.1038/nmeth871.
16. Willet N, Lamprecht C, Rankl C, Rangl M, Creasey R, Ebner R, Voelcker N, Hinterdorfer P. Molecular Recognition Force Spectroscopy. In: Molecular manipulation with atomic force microscopy: CRC Press; 2011. p. 3–46. https://doi.org/10.1201/b11269-3.
17. Almqvist N, Bhatia R, Primbs G, Desai N, Banerjee S, Lal R. Elasticity and adhesion force mapping reveals real-time clustering of growth factor receptors and associated changes in local cellular rheological properties. Biophys J. 2004;86(3):1753–62. https://doi.org/10.1016/S0006-3495(04)74243-5.
18. Alsteens D, Trabelsi H, Soumillion P, Dufrene YF. Multiparametric atomic force microscopy imaging of single bacteriophages extruding from living bacteria. Nat Commun. 2013;4:2926. https://doi.org/10.1038/ncomms3926.
19. Dupres V, Menozzi FD, Locht C, Clare BH, Abbott NL, Cuenot S, Bompard C, Raze D, Dufrene YF. Nanoscale mapping and functional analysis of individual adhesins on living bacteria. Nat Methods. 2005;2(7):515–20. https://doi.org/10.1038/nmeth769.
20. Gad M, Itoh A, Ikai A. Mapping cell wall polysaccharides of living microbial cells using atomic force microscopy. Cell Biol Int. 1997;21(11):697–706. https://doi.org/10.1006/cbir.1997.0214.
21. Ando T, Kodera N, Takai E, Maruyama D, Saito K, Toda A. A high-speed atomic force microscope for studying biological macromolecules. Proc Natl Acad Sci U S A. 2001;98(22):12468–72. https://doi.org/10.1073/pnas.211400898.
22. Takenaka M, Miyachi Y, Ishii J, Ogino C, Kondo A. The mapping of yeast's G-protein coupled receptor with an atomic force microscope. Nanoscale. 2015;7(11):4956–63. https://doi.org/10.1039/c4nr05940a.
23. Sahin O, Erina N. High-resolution and large dynamic range nanomechanical mapping in tapping-mode atomic force microscopy. Nanotechnology. 2008;19(44):445717. https://doi.org/10.1088/0957-4484/19/44/445717.
24. Raman A, Trigueros S, Cartagena A, Stevenson AP, Susilo M, Nauman E, Contera SA. Mapping nanomechanical properties of live cells using multi-harmonic atomic force microscopy. Nat Nanotechnol. 2011;6(12):809–14. https://doi.org/10.1038/nnano.2011.186.
25. Cartagena-Rivera AX, Wang WH, Geahlen RL, Raman A. Fast, multi-frequency, and quantitative nanomechanical mapping of live cells using the atomic force microscope. Sci Rep. 2015;5:11692. https://doi.org/10.1038/srep11692.

26. Chirasatitsin S, Engler AJ. Detecting cell-adhesive sites in extracellular matrix using force spectroscopy mapping. J Phys Condens Matter. 2010;22(19):194102. https://doi.org/10.1088/0953-8984/22/19/194102.
27. Whitehead B, Wu L, Hvam ML, Aslan H, Dong M, Dyrskjot L, Ostenfeld MS, Moghimi SM, Howard KA. Tumour exosomes display differential mechanical and complement activation properties dependent on malignant state: implications in endothelial leakiness. J Extracellular Vesicles. 2015;4:29685. https://doi.org/10.3402/jev.v4.29685.
28. Zhang S, Aslan H, Besenbacher F, Dong M. Quantitative biomolecular imaging by dynamic nanomechanical mapping. Chem Soc Rev. 2014;43(21):7412–29. https://doi.org/10.1039/c4cs00176a.
29. Pletikapic G, Berquand A, Radic TM, Svetlicic V. Quantitative Nanomechanical mapping of marine diatom in seawater using peak force tapping atomic force microscopy(1). J Phycol. 2012;48(1):174–85. https://doi.org/10.1111/j.1529-8817.2011.01093.x.
30. Picas L, Rico F, Scheuring S. Direct measurement of the mechanical properties of lipid phases in supported bilayers. Biophys J. 2012;102(1):L01–3. https://doi.org/10.1016/j.bpj.2011.11.4001.
31. Medalsy I, Hensen U, Muller DJ. Imaging and quantifying chemical and physical properties of native proteins at molecular resolution by force-volume AFM. Angew Chem. 2011;50(50):12103–8. https://doi.org/10.1002/anie.201103991.
32. Pfreundschuh M, Hensen U, Muller DJ. Quantitative imaging of the electrostatic field and potential generated by a transmembrane protein pore at subnanometer resolution. Nano Lett. 2013;13(11):5585–93. https://doi.org/10.1021/nl403232z.
33. Rico F, Su C, Scheuring S. Mechanical mapping of single membrane proteins at submolecular resolution. Nano Lett. 2011;11(9):3983–6. https://doi.org/10.1021/nl202351t.
34. Chopinet L, Formosa C, Rols MP, Duval RE, Dague E. Imaging living cells surface and quantifying its properties at high resolution using AFM in QI mode. Micron. 2013;48:26–33. https://doi.org/10.1016/j.micron.2013.02.003.
35. Carrasco C, Carreira A, Schaap IA, Serena PA, Gomez-Herrero J, Mateu MG, de Pablo PJ. DNA-mediated anisotropic mechanical reinforcement of a virus. Proc Natl Acad Sci U S A. 2006;103(37):13706–11. https://doi.org/10.1073/pnas.0601881103.
36. Gunning AP, Chambers S, Pin C, Man AL, Morris VJ, Nicoletti C. Mapping specific adhesive interactions on living human intestinal epithelial cells with atomic force microscopy. FASEB J. 2008;22(7):2331–9. https://doi.org/10.1096/fj.07-100578.
37. Heu C, Berquand A, Elie-Caille C, Nicod L. Glyphosate-induced stiffening of HaCaT keratinocytes, a peak force tapping study on living cells. J Struct Biol. 2012;178(1):1–7. https://doi.org/10.1016/j.jsb.2012.02.007.
38. Li M, Liu L, Xi N, Wang Y, Xiao X, Zhang W. Imaging and measuring the biophysical properties of Fc gamma receptors on single macrophages using atomic force microscopy. Biochem Biophys Res Commun. 2013;438(4):709–14. https://doi.org/10.1016/j.bbrc.2013.07.114.
39. Li M, Xiao X, Liu L, Xi N, Wang Y, Dong Z, Zhang W. Nanoscale mapping and organization analysis of target proteins on cancer cells from B-cell lymphoma patients. Exp Cell Res. 2013;319(18):2812–21. https://doi.org/10.1016/j.yexcr.2013.07.020.
40. Saab MB, Bec N, Martin M, Estephan E, Cuisinier F, Larroque C, Gergely C. Differential effect of curcumin on the nanomechanics of normal and cancerous Mammalian epithelial cells. Cell Biochem Biophys. 2013;65(3):399–411. https://doi.org/10.1007/s12013-012-9443-1.
41. Wegmann S, Medalsy ID, Mandelkow E, Muller DJ. The fuzzy coat of pathological human Tau fibrils is a two-layered polyelectrolyte brush. Proc Natl Acad Sci U S A. 2013;110(4):E313–21. https://doi.org/10.1073/pnas.1212100110.
42. Willemsen OH, Snel MM, van der Werf KO, de Grooth BG, Greve J, Hinterdorfer P, Gruber HJ, Schindler H, van Kooyk Y, Figdor CG. Simultaneous height and adhesion imaging of antibody-antigen interactions by atomic force microscopy. Biophys J. 1998;75(5):2220–8. https://doi.org/10.1016/S0006-3495(98)77666-0.

43. Canale C, Jacono M, Diaspro A, Dante S. Force spectroscopy as a tool to investigate the properties of supported lipid membranes. Microsc Res Tech. 2010;73(10):965–72. https://doi.org/10.1002/jemt.20834.
44. Cinar G, Ceylan H, Urel M, Erkal TS, Deniz Tekin E, Tekinay AB, Dana A, Guler MO. Amyloid inspired self-assembled peptide nanofibers. Biomacromolecules. 2012;13(10):3377–87. https://doi.org/10.1021/bm301141h.
45. Vasilev C, Brindley AA, Olsen JD, Saer RG, Beatty JT, Hunter CN. Nano-mechanical mapping of the interactions between surface-bound RC-LH1-PufX core complexes and cytochrome c 2 attached to an AFM probe. Photosynth Res. 2014;120(1–2):169–80. https://doi.org/10.1007/s11120-013-9812-7.
46. Kim IH, Lee MN, Ryu SH, Park JW. Nanoscale mapping and affinity constant measurement of signal-transducing proteins by atomic force microscopy. Anal Chem. 2011;83(5):1500–3. https://doi.org/10.1021/ac102695e.
47. Wang C, Yadavalli VK. Spatial recognition and mapping of proteins using DNA aptamers. Nanotechnology. 2014;25(45):455101. https://doi.org/10.1088/0957-4484/25/45/455101.
48. Dorakumbura BN, Becker T, Lewis SW. Nanomechanical mapping of latent fingermarks: a preliminary investigation into the changes in surface interactions and topography over time. Forensic Sci Int. 2016;267:16–24. https://doi.org/10.1016/j.forsciint.2016.07.024.
49. Rigato A, Rico F, Eghiaian F, Piel M, Scheuring S. Atomic force microscopy mechanical mapping of micropatterned cells shows adhesion geometry-dependent mechanical response on local and global scales. ACS Nano. 2015;9(6):5846–56. https://doi.org/10.1021/acsnano.5b00430.
50. Francius G, Alsteens D, Dupres V, Lebeer S, De Keersmaecker S, Vanderleyden J, Gruber HJ, Dufrene YF. Stretching polysaccharides on live cells using single molecule force spectroscopy. Nat Protoc. 2009;4(6):939–46. https://doi.org/10.1038/nprot.2009.65.
51. Dupres V, Alsteens D, Andre G, Dufrene YF. Microbial nanoscopy: a closer look at microbial cell surfaces. Trends Microbiol. 2010;18(9):397–405. https://doi.org/10.1016/j.tim.2010.06.004.
52. Dague E, Alsteens D, Latge JP, Verbelen C, Raze D, Baulard AR, Dufrene YF. Chemical force microscopy of single live cells. Nano Lett. 2007;7(10):3026–30. https://doi.org/10.1021/nl071476k.
53. Marliere C, Dhahri S. An in vivo study of electrical charge distribution on the bacterial cell wall by atomic force microscopy in vibrating force mode. Nanoscale. 2015;7(19):8843–57. https://doi.org/10.1039/c5nr00968e.
54. El-Kirat-Chatel S, Beaussart A, Derclaye S, Alsteens D, Kucharikova S, Van Dijck P, Dufrene YF. Force nanoscopy of hydrophobic interactions in the fungal pathogen Candida glabrata. ACS Nano. 2015;9(2):1648–55. https://doi.org/10.1021/nn506370f.
55. Formosa C, Schiavone M, Boisrame A, Richard ML, Duval RE, Dague E. Multiparametric imaging of adhesive nanodomains at the surface of Candida albicans by atomic force microscopy. Nanomedicine (NBM). 2015;11(1):57–65. https://doi.org/10.1016/j.nano.2014.07.008.
56. Cartagena A, Hernando-Perez M, Carrascosa JL, de Pablo PJ, Raman A. Mapping in vitro local material properties of intact and disrupted virions at high resolution using multi-harmonic atomic force microscopy. Nanoscale. 2013;5(11):4729–36. https://doi.org/10.1039/c3nr34088k.
57. Osada T, Itoh A, Ikai A. Mapping of the Receptor-Associated Protein (RAP) binding proteins on living fibroblast cells using an atomic force microscope. Ultramicroscopy. 2003;97(1–4):353–7. https://doi.org/10.1016/S0304-3991(03)00060-3.
58. Osada T, Takezawa S, Itoh A, Arakawa H, Ichikawa M, Ikai A. The distribution of sugar chains on the vomeronasal epithelium observed with an atomic force microscope. Chem Senses. 1999;24(1):1–6.
59. Kuznetsova TG, Starodubtseva MN, Yegorenkov NI, Chizhik SA, Zhdanov RI. Atomic force microscopy probing of cell elasticity. Micron. 2007;38(8):824–33. https://doi.org/10.1016/j.micron.2007.06.011.

60. Efremov YM, Dzyubenko EV, Bagrov DV, Maksimov GV, Shram SI, Shaitan KV. Atomic force microscopy study of the arrangement and mechanical properties of astrocytic cytoskeleton in growth medium. Acta Nat. 2011;3(3):93–9.
61. Cassina V, Torsello A, Tempestini A, Salerno D, Brogioli D, Tamiazzo L, Bresciani E, Martinez J, Fehrentz JA, Verdie P, Omeljaniuk RJ, Possenti R, Rizzi L, Locatelli V, Mantegazza F. Biophysical characterization of a binding site for TLQP-21, a naturally occurring peptide which induces resistance to obesity. Biochim Biophys Acta. 2013;1828(2):455–60. https://doi.org/10.1016/j.bbamem.2012.10.023.
62. Kawas LH, Benoist CC, Harding JW, Wayman GA, Abu-Lail NI. Nanoscale mapping of the met receptor on hippocampal neurons by AFM and confocal microscopy. Nanomedicine (NBM). 2013;9(3):428–38. https://doi.org/10.1016/j.nano.2012.08.008.
63. Wang B, Guo P, Auguste DT. Mapping the CXCR4 receptor on breast cancer cells. Biomaterials. 2015;57:161–8. https://doi.org/10.1016/j.biomaterials.2015.04.023.
64. Ebner A, Kienberger F, Kada G, Stroh CM, Geretschlager M, Kamruzzahan AS, Wildling L, Johnson WT, Ashcroft B, Nelson J, Lindsay SM, Gruber HJ, Hinterdorfer P. Localization of single avidin-biotin interactions using simultaneous topography and molecular recognition imaging. ChemPhysChem. 2005;6(5):897–900. https://doi.org/10.1002/cphc.200400545.
65. Stroh C, Wang H, Bash R, Ashcroft B, Nelson J, Gruber H, Lohr D, Lindsay SM, Hinterdorfer P. Single-molecule recognition imaging microscopy. Proc Natl Acad Sci U S A. 2004;101(34):12503–7. https://doi.org/10.1073/pnas.0403538101.
66. Stroh CM, Ebner A, Geretschlager M, Freudenthaler G, Kienberger F, Kamruzzahan AS, Smith-Gill SJ, Gruber HJ, Hinterdorfer P. Simultaneous topography and recognition imaging using force microscopy. Biophys J. 2004;87(3):1981–90. https://doi.org/10.1529/biophysj.104.043331.
67. Raab A, Han W, Badt D, Smith-Gill SJ, Lindsay SM, Schindler H, Hinterdorfer P. Antibody recognition imaging by force microscopy. Nat Biotechnol. 1999;17(9):901–5. https://doi.org/10.1038/12898.
68. Ebner A, Wildling L, Kamruzzahan AS, Rankl C, Wruss J, Hahn CD, Holzl M, Zhu R, Kienberger F, Blaas D, Hinterdorfer P, Gruber HJ. A new, simple method for linking of antibodies to atomic force microscopy tips. Bioconjug Chem. 2007;18(4):1176–84. https://doi.org/10.1021/bc070030s.
69. Ebner A, Wildling L, Zhu R, Rankl C, Haselgrubler T, Hinterdorfer P, Gruber HJ. Functionalization of probe tips and supports for single-molecule recognition force microscopy. Top Curr Chem. 2008;285:29–76. https://doi.org/10.1007/128_2007_24.
70. Kamruzzahan AS, Ebner A, Wildling L, Kienberger F, Riener CK, Hahn CD, Pollheimer PD, Winklehner P, Holzl M, Lackner B, Schorkl DM, Hinterdorfer P, Gruber HJ. Antibody linking to atomic force microscope tips via disulfide bond formation. Bioconjug Chem. 2006;17(6):1473–81. https://doi.org/10.1021/bc060252a.
71. Preiner J, Ebner A, Chtcheglova L, Zhu R, Hinterdorfer P. Simultaneous topography and recognition imaging: physical aspects and optimal imaging conditions. Nanotechnology. 2009;20(21):215103. https://doi.org/10.1088/0957-4484/20/21/215103.
72. Preiner J, Losilla NS, Ebner A, Annibale P, Biscarini F, Garcia R, Hinterdorfer P. Imaging and detection of single molecule recognition events on organic semiconductor surfaces. Nano Lett. 2009;9(2):571–5. https://doi.org/10.1021/nl802721g.
73. Ron A, Singh RR, Fishelson N, Socher R, Benayahu D, Shacham-Diamand Y. Site localization of membrane-bound proteins on whole cell level using atomic force microscopy. Biophys Chem. 2008;132(2–3):127–38. https://doi.org/10.1016/j.bpc.2007.10.016.
74. Zhao W, Liu S, Cai M, Xu H, Jiang J, Wang H. Detection of carbohydrates on the surface of cancer and normal cells by topography and recognition imaging. Chem Commun. 2013;49(29):2980–2. https://doi.org/10.1039/c3cc38885a.
75. Tang J, Ebner A, Badelt-Lichtblau H, Vollenkle C, Rankl C, Kraxberger B, Leitner M, Wildling L, Gruber HJ, Sleytr UB, Ilk N, Hinterdorfer P. Recognition imaging and highly ordered molecular templating of bacterial S-layer nanoarrays containing affinity-tags. Nano Lett. 2008;8(12):4312–9. https://doi.org/10.1021/nl802092c.

76. Ebner A, Nikova D, Lange T, Haberle J, Falk S, Dubbers A, Bruns R, Hinterdorfer P, Oberleithner H, Schillers H. Determination of CFTR densities in erythrocyte plasma membranes using recognition imaging. Nanotechnology. 2008;19(38):384017. https://doi.org/10.1088/0957-4484/19/38/384017.
77. Chtcheglova LA, Atalar F, Ozbek U, Wildling L, Ebner A, Hinterdorfer P. Localization of the ergtoxin-1 receptors on the voltage sensing domain of hERG K channel by AFM recognition imaging. Pflugers Arch: Eur J Physiol. 2008;456(1):247–54. https://doi.org/10.1007/s00424-007-0418-9.
78. Chtcheglova LA, Waschke J, Wildling L, Drenckhahn D, Hinterdorfer P. Nano-scale dynamic recognition imaging on vascular endothelial cells. Biophys J. 2007;93(2):L11–3. https://doi.org/10.1529/biophysj.107.109751.
79. Radmacher M, Cleveland JP, Fritz M, Hansma HG, Hansma PK. Mapping interaction forces with the atomic force microscope. Biophys J. 1994;66(6):2159–65. https://doi.org/10.1016/S0006-3495(94)81011-2.
80. Ludwig M, Dettmann W, Gaub HE. Atomic force microscope imaging contrast based on molecular recognition. Biophys J. 1997;72(1):445–8. https://doi.org/10.1016/S0006-3495(97)78685-5.
81. Agnihotri A, Siedlecki CA. Adhesion mode atomic force microscopy study of dual component protein films. Ultramicroscopy. 2005;102(4):257–68. https://doi.org/10.1016/j.ultramic.2004.10.006.
82. Wang H, Bash R, Lohr D. Two-component atomic force microscopy recognition imaging of complex samples. Anal Biochem. 2007;361(2):273–9. https://doi.org/10.1016/j.ab.2006.11.039.
83. van Es MH, Tang J, Preiner J, Hinterdorfer P, Oosterkamp TH. Single molecule binding dynamics measured with atomic force microscopy. Ultramicroscopy. 2014;140:32–6. https://doi.org/10.1016/j.ultramic.2014.02.005.
84. Hecht FM, Rheinlaender J, Schierbaum N, Goldmann WH, Fabry B, Schaffer TE. Imaging viscoelastic properties of live cells by AFM: power-law rheology on the nanoscale. Soft Matter. 2015;11(23):4584–91. https://doi.org/10.1039/c4sm02718c.
85. Kumar U, Vivekanand K, Poddar P. Real-time nanomechanical and topographical mapping on live bacterial cells-Brevibacterium casei under stress due to their exposure to Co_2 ions during microbial synthesis of Co_3O_4 nanoparticles. J Phys Chem B. 2009;113(22):7927–33. https://doi.org/10.1021/jp902698n.
86. Chtcheglova LA, Hinterdorfer P. Atomic force microscopy functional imaging on vascular endothelial cells. Methods Mol Biol. 2013;931:331–44. https://doi.org/10.1007/978-1-62703-056-4_16.
87. Leitner M, Poturnayova A, Lamprecht C, Weich S, Snejdarkova M, Karpisova I, Hianik T, Ebner A. Characterization of the specific interaction between the DNA aptamer sgc8c and protein tyrosine kinase-7 receptors at the surface of T-cells by biosensing AFM. Anal Bioanal Chem. 2017;409(11):2767–76. https://doi.org/10.1007/s00216-017-0238-5.
88. Takahashi H, Hizume K, Kumeta M, S HY, Takeyasu K (2009) Single-molecule anatomy by atomic force microscopy and recognition imaging. Arch Histol Cytol 72 (4–5):217–225.
89. Hu Y, Ulstrup J, Zhang J, Molin S, Dupres V. Adhesive properties of Staphylococcus epidermidis probed by atomic force microscopy. Phys Chem Chem Phys. 2011;13(21):9995–10003. https://doi.org/10.1039/c0cp02800b.
90. Mochizuki M, Oguchi M, Kim SO, Jackman JA, Ogawa T, Lkhamsuren G, Cho NJ, Hayashi T. Quantitative evaluation of peptide-material interactions by a force mapping method: guidelines for surface modification. Langmuir. 2015;31(29):8006–12. https://doi.org/10.1021/acs.langmuir.5b01691.
91. Zhu R, Ebner A, Kastner M, Preiner J, Howorka S, Hinterdorfer P. Topography and recognition imaging of protein-patterned surfaces generated by AFM nanolithography. ChemPhysChem. 2009;10(9–10):1478–81. https://doi.org/10.1002/cphc.200900245.

92. Knittel P, Mizaikoff B, Kranz C. Simultaneous Nanomechanical and electrochemical mapping: combining peak force tapping atomic force microscopy with scanning electrochemical microscopy. Anal Chem. 2016;88(12):6174–8. https://doi.org/10.1021/acs.analchem.6b01086.
93. Alsteens D, Garcia MC, Lipke PN, Dufrene YF. Force-induced formation and propagation of adhesion nanodomains in living fungal cells. Proc Natl Acad Sci U S A. 2010;107(48):20744–9. https://doi.org/10.1073/pnas.1013893107.
94. Hinterdorfer P, Garcia-Parajo MF, Dufrene YF. Single-molecule imaging of cell surfaces using near-field nanoscopy. Acc Chem Res. 2012;45(3):327–36. https://doi.org/10.1021/ar2001167.